

# Design of photonic band gap in one-dimensional SiO<sub>2</sub>/a-Si photonic crystals

SAHAR A. EL-NAGGAR\*, NADIA H. RAFAT, SAMIA I. MOSTAFA

*Dept. of Engineering Math. and Physics, Faculty of Engineering, Cairo University, Giza, Egypt*

We theoretically study one dimensional binary SiO<sub>2</sub>/a-Si photonic crystals taking into consideration the dissipative nature of amorphous Si. We suggest a method namely; "modified thickness" to control the band gaps central frequencies by gradually changing the width of the alternating layers. We calculate the reflectance, transmittance and absorbance of light based on the transfer matrix method. Calculations show that photonic band gaps can occur at the suggested central frequency and its multiples. We discuss the limitations on the choice of the first central band gap frequency, thickness of the a-Si layers and number of periods.

(Received May 5, 2011; accepted July 25, 2011)

*Keywords:* Photonic crystals; one-dimensional; Modified structure; Amorphous Si, Silicon Dioxide

## 1. Introduction

An enormous range of technological developments would become possible if we could engineer materials that respond to light waves over a desired range of frequencies by perfectly reflecting them [1]. One of the most important and useful property of photonic crystals (PCs) is the existence of photonic band gaps (PBGs), the range of energy where no electromagnetic modes can exist. These electromagnetic waves with frequencies located in the PBG cannot propagate in the PCs due to multiple Bragg scattering.

One-dimensional photonic crystals (PCs) are periodic structures stacked by alternating different materials with distinct refractive indices. Although the 1-D PCs are the simplest among 2-D and 3-D, from both the theoretical and fabrication point of view, they have properties and applications as important as 2-D and 3-D PCs. Simple 1-D dielectric-dielectric photonic crystals (DDPCs) [2-4] and metal-dielectric photonic crystals (MDPCs) [5-7] play an important role in modern photonics. They are easily fabricated by modern experimental techniques. They are utilized as high-reflection mirrors and antireflection coatings [8]. However, for the GaAs/air PCs [2], Si/SiO<sub>2</sub> PCs [3] and poly-Si/SiO<sub>2</sub> PC [4], the dissipative nature of the semiconductor layers was neglected. Most of the work done in this field focuses on PBG enlargement that suggested to be enlarged by increasing the refractive index contrast in the constituent materials, using disordered PCs [9-10], using graded dielectric layers [3] and using heterostructured PCs [11].

In this work we focus our attention on DDPCs as a stack of SiO<sub>2</sub>/ a-Si layers. The effect of the absorption of light in the a-Si layers, which was neglected in some previously published work, is taken into consideration in the calculations. We suggest a modified thickness structure that changes the dielectric thickness gradually in a way different than previously published work. We

increase the thicknesses of the SiO<sub>2</sub> gradually and decrease the thicknesses of the a-Si gradually to control the PBGs. SiO<sub>2</sub> represents the low refractive index material while a-Si represents the high refractive index material. The large refractive index contrast at the SiO<sub>2</sub>/a-Si interface produces a high reflectance. It is technologically possible to produce such structure having thickness of the nanometer scale [12-14].

This paper is organized as follows: section 2 contains the structure suggested and the basic equations used. Section 3 contains calculations and results and is divided into two subsections. In subsection 3.1, we present the calculations and results of producing PBGs assuming lossless a-Si. In subsection 3.2, the dissipative nature of the a-Si is considered and the absorbance is calculated. In the conclusion section, the effect of absorption and the limitations on the choice of the central frequency are discussed.

## 2. Structure and basic equations

In this work we suggest a PC of stacked SiO<sub>2</sub>/ a-Si layers inserted between an incidence region of refractive index  $n_o$  and a substrate region of refractive index  $n_s$  as shown in fig. 1. The PC unit cell of lattice parameter,  $a = d_1 + d_2$ , consists of a SiO<sub>2</sub> layer of width  $d_1$  having a refractive index  $n_1$  and an a-Si layer of width  $d_2$  having a refractive index  $n_2$ . This unit cell is repeated  $N$  times to construct the PC. We assume normal incidence of electromagnetic waves and thus the electric and magnetic fields directions are parallel (tangent) to the interface. The electric field in the  $j$ -th layer can be written as:

$$E_j = a_j \exp(in_j k(x - x_j)) + b_j \exp(-in_j k(x - x_j)) \quad (1)$$

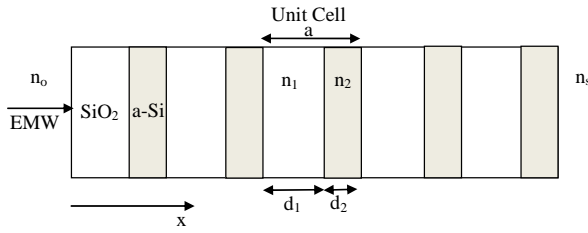


Fig. 1. A schematic of the  $\text{SiO}_2/\text{a-Si}$  1-D PC. The refractive index of the incidence region is  $n_o$ , and  $n_s$  is the index of the substrate region.

Where:  $x_j$  is the coordinate of the  $j$ -th interface. The amplitude of the right and the left propagating wave in the  $j$ -th layer are  $a_j$  and  $b_j$  respectively.  $k$  is the free-space wave number and equals  $2\pi/\lambda$  and  $\lambda$  is the wavelength in free space.

The electric and the magnetic field can be arranged in a matrix form as:

$$\begin{bmatrix} E_j \\ B_j \end{bmatrix} = \begin{bmatrix} \exp(in_j k(x-x_j)) & \exp(-in_j k(x-x_j)) \\ n_j \exp(in_j k(x-x_j)) & -n_j \exp(-in_j k(x-x_j)) \end{bmatrix} \begin{bmatrix} a_j \\ b_j \end{bmatrix} \quad (2)$$

We define a layer propagation transfer matrix  $\tau_j$  of the  $j$ -th layer as the matrix that relates the electric and the magnetic fields that lie in the left boundary plane (at  $x = x_j$ ) to those in its right boundary plane (at  $x = x_j + d_j$ ). Thus,  $\tau_j$  of the  $j$ -th layer of refractive index  $n_j$  and thickness  $d_j$  can be written as:

$$\tau_j = \begin{bmatrix} \exp(in_j kd_j) & \exp(-in_j kd_j) \\ n_j \exp(in_j kd_j) & -n_j \exp(-in_j kd_j) \end{bmatrix} \begin{bmatrix} 1 & 1 \\ n_j & -n_j \end{bmatrix}^{-1} \quad (3)$$

which can be simplified to:

$$\tau_j = \begin{bmatrix} \cos(n_j kd_j) & i n_j^{-1} \sin(n_j kd_j) \\ i n_j \sin(n_j kd_j) & \cos(n_j kd_j) \end{bmatrix} \quad (4)$$

The condition of continuity of the tangential components of the electric and magnetic field across an interface together with the assumption of normal incidence conclude that the fields at  $x = x_j + d_j$  of the  $j$ -th layer equal those at  $x = x_{j+1}$  of  $(j+1)$  layer. Thus, the transfer matrix for the whole structure will be the product of the transfer matrices of the layers in the appropriate order defined by equation (4). The final form of the equations can be written as follows:

$$\begin{bmatrix} a_s \\ b_s \end{bmatrix} = \begin{bmatrix} T_{11} & T_{12} \\ T_{21} & T_{22} \end{bmatrix} \begin{bmatrix} a_o \\ b_o \end{bmatrix} \quad (5)$$

The subscripts “s” and “o” refer to the substrate and the incidence regions respectively. The amplitude of the right propagating wave in the incidence region,  $a_o$  is set to unity and the amplitude of the left propagating wave in the substrate,  $b_s$ , is set to zero. Thus, the amplitude of the right propagating wave in the substrate,  $a_s$ , and the amplitude of the left propagating wave in the incidence region,  $b_o$ , represent the transmission and the reflection coefficients respectively. These coefficients can be derived from the elements of the transfer matrix as:

$$b_o = -T_{21}/T_{22} \quad a_s = T_{11} - T_{12}T_{21}/T_{22} \quad (6)$$

The associated transmittance  $T$  and reflectance  $R$  are calculated from  $T = n_s |a_s|^2 / n_o$  and  $R = |b_o|^2$ . Finally, the absorbance  $A$  can be obtained from

$$A = 1 - R - T \quad (7)$$

### 3. Calculations and results

In the following analysis, the incidence region is assumed to be air with refractive index  $n_o = 1$  and the substrate is assumed to be semi-infinite air with refractive index  $n_s = 1$ . The calculations are done assuming lossless a-Si with no absorption of electromagnetic wave throughout the a-Si layers. Then the calculations are repeated taking into consideration the imaginary part of the refractive index which indicates absorption through the a-Si layers that affects the optical response.

#### 3.1 Lossless a-Si

In this part of the calculations, we neglect the absorption in the a-Si layers. Hence, the refractive index of the a-Si is taken to be real and frequency independent in the frequency range considered.

We started by assuming a quarter-wavelength  $\lambda_o/4$  stack. That is  $n_1 d_1 = n_2 d_2 = \lambda_o/4$  where  $\lambda_o$  is the suggested first band-gap central wavelength, taken as 2500 nm. The numerical values of the parameters used are summarized in Table I.

The dispersion relation of a 1-D binary layers can be expressed as [7]

$$\cos(qa) = \cos(k_1 d_1) \cos(k_2 d_2) - 0.5 \left( \frac{k_1}{k_2} + \frac{k_2}{k_1} \right) \sin(k_1 d_1) \sin(k_2 d_2) \quad (8)$$

where,  $q$  is the Bloch wave vector. The local wave vector is given by  $k_j = n_j \omega/c$  where  $n_j$  is the refractive index of the  $j$ -th layer.

Fig. 2 shows the band diagram for our  $\text{SiO}_2/\text{a-Si}$  calculated using equation (8), where,  $\omega_o$  is the central frequency. Two PBGs, centered at  $\omega_o$  (0.5eV) and  $3\omega_o$

(1.5eV), are noticed. In these gaps the wave vector is imaginary and the field decays.

The reflectance spectrum of 1D SiO<sub>2</sub>/a-Si PCs with 10 periods is shown in figure 3(a). Two band gaps are centered at  $\omega_0$  and  $3\omega_0$  in agreement with the photonic

band diagram shown previously in Figure 2. These gaps are in the frequency ranges  $0.7\omega_0 - 1.3\omega_0$  (0.35eV – 0.65eV) and  $2.7\omega_0 - 3.3\omega_0$  (1.35eV – 1.65eV) with width of each equals  $0.6\omega_0$  (0.3eV).

Table 1. The numerical values of the parameters

Case	Layer	d	n	N	$\Delta d$	Figure
Lossless a-Si $\lambda_0=2500$ nm $n d = \lambda_0/4$	SiO <sub>2</sub>	431 nm	1.45	10	0	2 3(a)
	a-Si	156 nm	4		0	
Lossless a-Si $\lambda_0=2500$ nm	SiO <sub>2</sub>	431 nm	1.45	10	47.8nm	3(b)
	a-Si	156 nm	4		-17.3nm	
Lossy a-Si $\lambda_0=2500$ nm	SiO <sub>2</sub>	431 nm	1.45	10	0	4
	a-Si	156 nm	$n(\omega)$ [15]		0	
Lossy a-Si $\lambda_0=2500$ nm	SiO <sub>2</sub>	431 nm	1.45	4, 6, 8	$d_1/(N-1)$	5
	a-Si	156 nm	$n(\omega)$ [15]	& 10	$-d_2/(N-1)$	

We suggest a method (modified thickness method) to introduce extra gaps at  $2\omega_0$  and  $4\omega_0$ . We increase the thickness of the SiO<sub>2</sub> layers, gradually with a step of  $\Delta d_1 = d_1/(N-1)$ , where N is the number of periods. We decrease the thickness of the a-Si layers, gradually with a step of  $\Delta d_2 = d_2/(N-1)$ . By applying this method, at the N<sup>th</sup> period, the thickness of the a-Si layer vanishes and the thickness of SiO<sub>2</sub> layer is doubled. The reflectance spectrum of the modified thicknesses structure is shown in figure 3 (b). The figure shows photonic band gaps at frequencies ranges  $0.73\omega_0 - 1.2\omega_0$ ,  $1.71\omega_0 - 2.2\omega_0$ ,  $2.7\omega_0 - 3.17\omega_0$  and  $3.65\omega_0 - 4.16\omega_0$ . Thus, PBGs are introduced at  $2\omega_0$  and  $4\omega_0$  in addition to those at  $\omega_0$  and  $3\omega_0$ . Thus, using the modified thickness method, we get four perfect PBGs rather than two got using the uniform stack of the binary SiO<sub>2</sub>/a-Si layers.

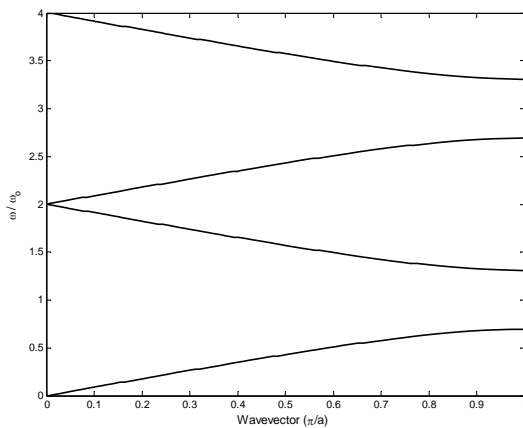


Fig. 2. The photonic band diagram based on quarter-wave ( $\lambda_0/4$ ) stack. The thicknesses of the SiO<sub>2</sub> and the a-Si layers are 431nm and 156 nm respectively.

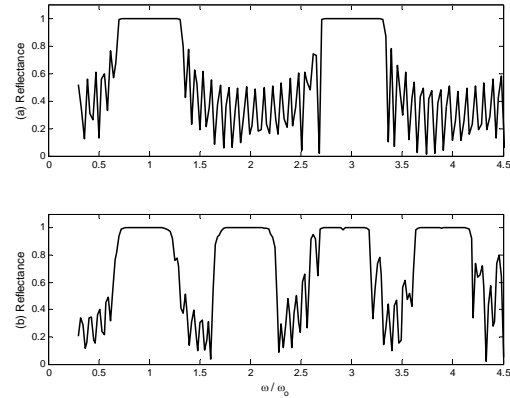


Fig. 3. The reflectance spectrum of the PC with 10 periods: (a)  $d_1$  and  $d_2$  are 431nm and 156 nm respectively, (b) modified thickness method with steps  $\Delta d_1 = 47.8$ nm and  $\Delta d_2 = -17.3$ nm respectively.

### 3.2 Lossy a-Si

In this part we deal with the a-Si material as a lossy medium, therefore the frequency dependence and the imaginary part of the refractive index of the a-Si are considered in our calculations in the range of wavelength  $< 1200$  nm. For range of wavelength greater than 1200 nm, the dependence on frequency is neglected and the imaginary part can be neglected with respect to the real part[15]. Fig. 4 shows the reflectance spectrum and the absorbance spectrum of 1D SiO<sub>2</sub>/a-Si PCs with 10 periods assuming  $\lambda_0 = 2500$  nm. For frequencies greater than  $3.3\omega_0$  or equivalently wavelength less than 675 nm, the absorption in the a-Si layers takes place that leads to reduction of reflectance below unity. At higher frequencies ( $\omega > 3.8\omega_0$ ), the reflectance oscillates with a peak around 0.5 and so does the absorbance. This leads to zero transmittance but not due to unity reflectance but due to around 50% reflectance and 50% absorbance.

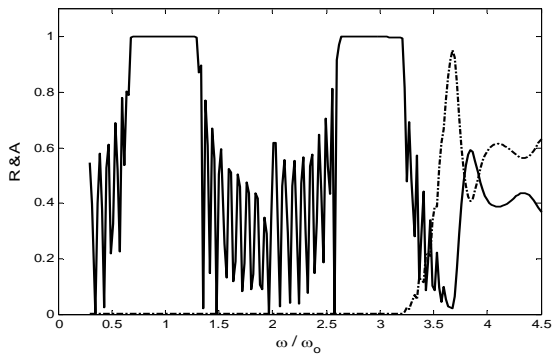


Fig. 4. The reflectance spectrum and the absorbance spectrum of the lossy a-Si PC with 10 periods plotted in solid lines and dash-dotted lines respectively.  $d_1$  and  $d_2$  are 431nm and 156 nm respectively.

Following the modified thickness method, described in the previous section, we increase the thicknesses of the SiO<sub>2</sub> gradually by a step of  $d_1/(N-1)$  and decrease the thicknesses of the a-Si gradually by a step of  $d_2/(N-1)$ . We repeat this for number of periods  $N = 4, 6, 8$  and 10. The reflectance spectrum and the absorbance spectrum are plotted in Figure 5. It is clear from the results that for few number of periods (e.g. 4), although we have ranges of frequencies with high reflectance  $> 90\%$ , but we cannot consider them as perfect PBGs. At these frequency ranges we still have percentage of transmittance. Increasing the number of periods (e.g. 10) leads to more perfect gaps with 100% reflectance and zero transmittance. The PBGs edges at such large number of periods show sharp transitions. The figure shows that only three PBGs at frequencies ranges  $(0.7\omega_0 - 1.19\omega_0)$ ,  $(1.7\omega_0 - 2.17\omega_0)$  and  $(2.65\omega_0 - 3.1\omega_0)$  can be realized. The unity reflectance, previously shown in figure 3(b), centered at  $4\omega_0$  vanishes because the absorbance in the a-Si layers around this frequency takes place especially for larger number of  $N$  due to the thicker a-Si layers for the wave to go through.

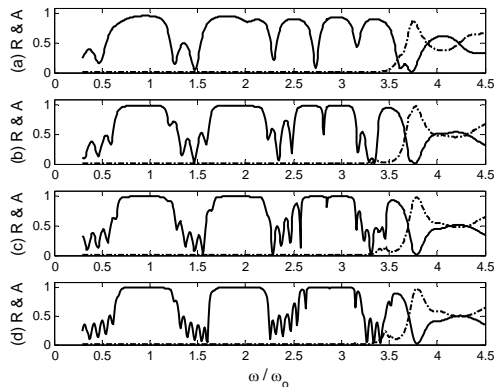


Fig. 5. The reflectance spectrum and the absorbance spectrum of the PC are plotted in solid lines and dash-dotted lines respectively (modified thickness method). (a)  $N=4$ , (b)  $N=6$ , (c)  $N=8$  and (d)  $N=10$ .

Fig. 6 shows the frequency ranges for possible PBGs that can be attained for the corresponding central wavelength  $\lambda_0$  using the modified thickness method. The calculations are done assuming  $n_1d_1 = n_2d_2 = \lambda_0/4$  to choose  $d_1$  and  $d_2$  (the widths of the first period of the stack). Then, the magnitude of  $\Delta d$  is calculated as  $\Delta d = d/(N-1)$  as done before. It is clear from the results that the number of bands decreases as the wavelength  $\lambda_0$  decreases. Only one PBG can be realized at  $\lambda_0$  range from 1250 nm to 600nm. That is in the visible-light range we cannot have more than one PBG. PBGs disappear at  $\lambda_0 < 500$  nm. We notice five wide PBGs at  $\lambda_0 = 4000$  nm. However, achieving such number of PBGs requires thicker a-Si and SiO<sub>2</sub> materials. That is the thicknesses of the first period of SiO<sub>2</sub> and a-Si using the quarter-wave should be 690nm and 250nm, respectively and the thickness of the SiO<sub>2</sub> will reach 1.38  $\mu\text{m}$  for the tenth period.

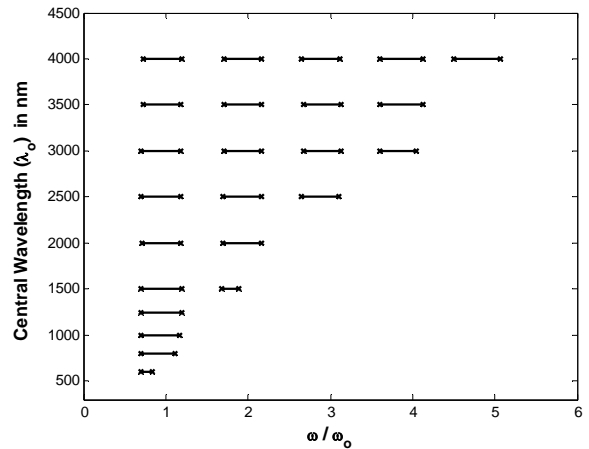


Fig. 6. The 100% reflectance bands of the 1D SiO<sub>2</sub>/a-Si PCs versus the central wavelength  $\lambda_0$  (modified thickness method).

In order to investigate the effect of the a-Si thickness on the PBGs width and position with respect to  $\omega_0$ , we vary the a-Si thickness from 15 nm in all periods to 160 nm in all periods. The thickness of the SiO<sub>2</sub> layer in each period is kept fixed at 431 nm. The number of periods is kept at ten, the number that gave us the best and enlarged form of bands in the previous analysis. Fig. 7 shows the variation of the PBGs position and width with the a-Si thickness. Increasing the a-Si thickness above 110 nm introduces a 3<sup>rd</sup> PBG that get wider as the a-Si thickness increases. We observe the broadening and then stability of the width of the first PBG as the a-Si thickness increases. On the other hand, the second PBG shows stability and then shrinkage as the a-Si increases. It is clear from the results that all the PBGs show red-shift as the thickness of the a-Si increases. The results show that the widest gaps occur in the range of 40 nm to 80 nm a-Si thickness. Since, a wide PBG is of necessity for the purpose of photonic applications, so for such 1D SiO<sub>2</sub>/a-Si PCs it is

better to limit the thickness of the a-Si layer between 40 nm and 80 nm.

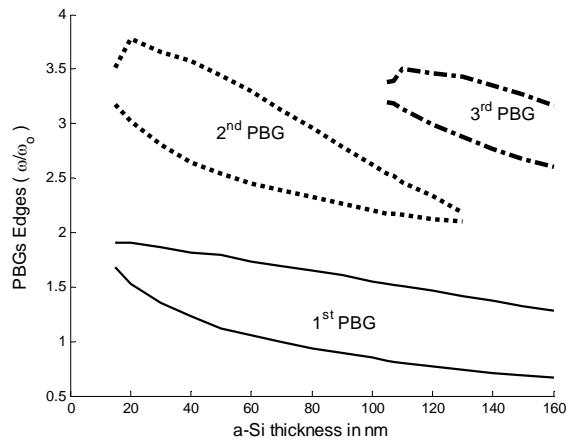


Fig. 7. The 100% reflectance bands of the 1D SiO<sub>2</sub>/a-Si PCs versus the a-Si thickness.

#### 4. Conclusion

The reflectance spectrum and the absorbance spectrum of binary SiO<sub>2</sub>/a-Si photonic crystals are investigated theoretically. Calculations show that, by gradually changing the thicknesses of PC layers, PBGs can occur at  $m\omega_0$ , where  $m$  is the PBG order and  $\omega_0$  is the first central frequency. Many PBGs can be realized at low frequencies. High absorption in the a-Si layers takes place in the high frequency range which limits the number of PBGs occurs. Only one PBG can be realized at  $\lambda_0$  range from 1250 nm to 600nm. PBG disappears at  $\lambda_0 < 500$  nm. PBGs can be adjusted by controlling the width of the a-Si layers. These PBGs show red-shift by increasing the width of the a-Si layers.

#### References

- [1] S.G.J. John D. Joannopoulos, Joshua N. Winn & Robert D. Meade, Photonic Crystals: Molding the Flow of Light (Second Edition), Princeton University Press, 2008.
- [2] Q. Zhu, D. Wang, Y. Zhang, Optik - International Journal for Light and Electron Optics, **122**, 330 (2011).

- [3] H. Tian, Y. Ji, C. Li, H. Liu, Optics Communications, **275**, 83-89 (2007).
- [4] M. Patrini, M. Galli, M. Belotti, L.C. Andreani, G. Guizzetti, G. Pucker, A. Lui, P. Bellutti, L. Pavesi, Journal of Applied Physics, **92**, 1816 (2002).
- [5] M.J. Keskinen, P. Loschialpo, D. Forester, J. Schelleng, Journal of Applied Physics **88**, 5785 (2000).
- [6] X. Xu, Y. Xi, D. Han, X. Liu, J. Zi, Z. Zhu, Applied Physics Letters, **86**, 091112-091112-091113 (2005).
- [7] Y.S. Junfei Yu, Xiaohan Liu, Rongtang Fu, Jian Zi Zhiqiang Zhu, Journal of Physics: Condensed Matter, **16**, L51-L56 (2004).
- [8] K. Sakoda, Optical Properties of Photonic Crystals (Second Edition), Springer-Verlag Berlin Heidelberg, 2005.
- [9] V.A. Tolmachev, T.S. Perova, J.A. Pilyugina, R.A. Moore, Optics Communications **259**, 104 (2006).
- [10] H. Li, H. Chen, X. Qiu, Physica B: Condensed Matter, **279**, 164 (2000).
- [11] X. Wang, X. Hu, Y. Li, W. Jia, C. Xu, X. Liu, J. Zi, Applied Physics Letters, **80**, 4291 (2002).
- [12] D.A. Muller, T. Sorsch, S. Moccio, F.H. Baumann, K. Evans-Lutterodt, G. Timp, Nature **399**, 758 (1999).
- [13] R. Sun, P. Dong, N.-n. Feng, C.-y. Hong, J. Michel, M. Lipson, L. Kimerling, Opt. Express, **15**, 17967 (2007).
- [14] Y.-B. Park, S.-W. Rhee, Journal of Applied Physics, **86**, 1346 (1999).
- [15] X. Ni, Z. Liu, A.V. Kildishev, PhotonicsDB: Optical Constants, 2007. DOI: 10254/nanohub-r3692.10, in.

\*Corresponding author: sel\_naggat@hotmail.com